IMPACT OF MINIATURIZATION ON THE CURRENT HANDLING OF ELECTROSTATIC MEMS RESONATORS

Manu Agarwal[1], Harsh Mehta[1], Robert N. Candler[2], Saurabh A. Chandorkar[1], Bongsang Kim[1], Matthew A. Hopcroft[1], Renata Melamud[1], Gaurav Bahl[1], Gary Yama[2], Thomas W. Kenny[1] and Boris Murmann[1]

[1]Departments of Electrical and Mechanical Eng., Stanford University, Stanford, CA, USA
[2]Robert Bosch Corporation (Research & Technology Center), Palo Alto, CA, USA

ABSTRACT

This paper studies the scaling of nonlinearities with miniaturization in double-ended-tuning-fork (DETF) MEMS resonators. We find that the increase in resonant frequency associated with beam length reduction strongly improves current handling; e.g. shortening the beams by a factor of 5 results in a 100-fold increase in sustainable signal current. Using the nonlinear models and scaling observed in this work, we present considerations for optimization of the resonant structure design and the electrostatic gap size.

1. INTRODUCTION

Electrostatic MEMS resonators have become an attractive and viable alternative to quartz crystal resonators, especially for timing/frequency reference applications [1]. Many of the advantages offered by these resonators, such as integration with CMOS, lower cost and low form factors will be more pronounced for smaller (miniaturized) micro-structure resonators.

High current handling is needed to attain large signal-to-noise-ratio in oscillator circuits tailored for precision frequency references. As in quartz, the current handling is limited by the amplitude-frequency (A-f) nonlinear effect [2]. This effect increases the relative far-from-carrier noise floor and also induces mixing of amplitude noise into close-to-carrier phase noise [3].

In this work, we study the impact of miniaturization on the nonlinear characteristics, and hence current handling, in electrostatically coupled MEMS resonators. The presented experimental results confirm existing models for the A-f effect [4] and provide design insight towards optimizing MEMS resonators for high precision frequency reference oscillators.

Fig. 1 shows a schematic of the resonant structure, the resonant mode shape, and a partial SEM cross section of the devices used in this study. The devices were fabricated using an epi-seal encapsulation process [5] using a <100> SOI wafer with a device layer thickness of $h = 20\ \mu m$ and an electrostatic gap size of $d = 1\ \mu m$. The beam lengths were oriented along the [110] direction. Fig. 2 shows the resonant frequencies (f_0) and quality factors (Q) of the measured devices.

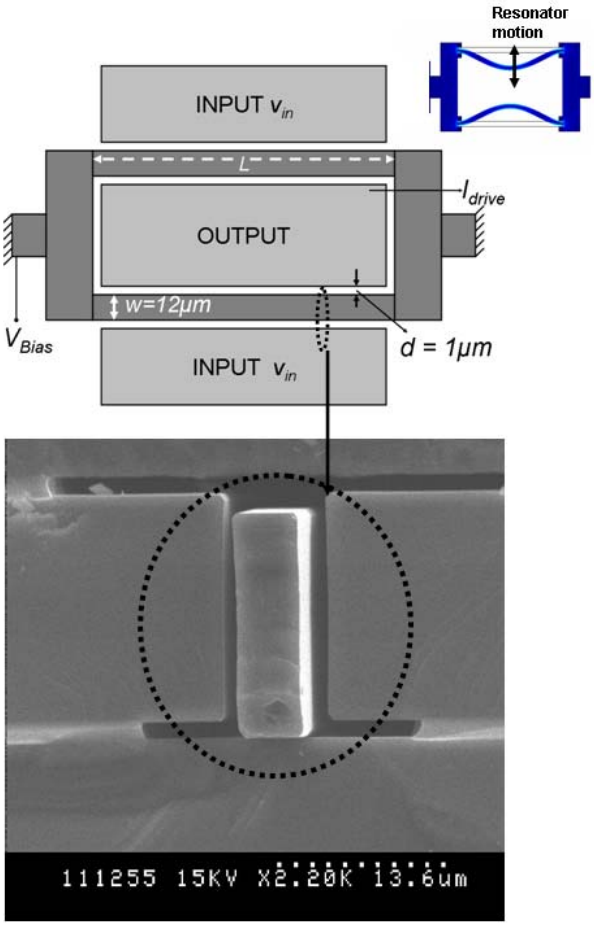

Fig. 1. Schematic showing the double ended tuning fork resonator with length L. The resonance mode is also shown, along with a partial SEM cross-section of the wafer scale encapsulated resonator.

2. THEORETICAL MODELS

In this section, we briefly summarize existing analytical models for the A-f effect and current handling [4, 6, 7]. Using the solution to the nonlinear equation for low damping oscillations [8], we can

define the A-f coefficient (κ) as

$$\frac{\Delta f}{f_0} = \kappa I_{drive}^2 \qquad (1)$$

The A-f effect causes distortion in the frequency response with increasing I_{drive} (see Fig. 3). Mechanical nonlinearities lead to stiffening, which causes right hand side bending of the response (Fig. 3(a)). At high bias voltages, electrical nonlinearities dominate and cause softening, which results in left hand side bending of the response (Fig. 3(b)).

Table 1 shows analytical model expressions for the parameters relevant to this discussion. Here, L and w are the beam length and beam width, E and ρ are the Young's modulus and the density of the beam material (single-crystal-silicon), respectively. m is the effective mass of the structure, ω_0 is the frequency of oscillation, A is the area of stimulus and pickup transduction and ε is the permittivity of the material in the structure-to-electrode gap. β^2 is the mode constant, equal to 4.73 for the mode of vibration and Q is the resonator's quality factor. Due to the complex nature of the involved energy loss mechanisms, there is no simple relationship that describes the dependence of Q on L (Fig. 2) [9, 10]. We hence treat Q as an independent parameter.

In these resonators it is possible to balance the electrical and mechanical nonlinearities by operating at $V_{Bias,opt}$ [6]. $I_{drive,opt}$ is the maximum bifurcation limited current handling at $V_{Bias,opt}$. A conservative (lower-bound) estimate for this can be obtained using κ_e in the expression for $I_{drive,opt}$ given in Table 1.

As can be seen from Table 1, k_3, κ_e and $V_{Bias,opt}$ are independent of Q, only the expression for current handling ($I_{drive,opt}$) shows a dependence on quality factor. The beam length dependence of all parameters under consideration is summarized in the rightmost column of Table 1. In the remainder of this paper, these dependencies will be verified experimentally.

3. RESULTS

Fig. 4 shows a typical dependence of $\kappa = \kappa_m + \kappa_e$ on V_{Bias}. κ was extracted from peak frequency vs. peak drive current data using a parabolic fit at each bias voltage. These measurements were repeated for each resonator with different beam lengths.

Fig. 5 shows measured k_3 for different beam lengths, along with theoretical calculations [7] and FEM simulation results. The measurements exhibit the theoretically predicted L^{-3} scaling, and shows a good match with the models, which had not been experimentally verified previously for beam type resonators. The FEM simulation results shown in Fig. 5 were obtained using the structural mechanics (plane stress), static nonlinear analysis module (parametric) in COMSOL® [11].

Fig. 6 shows the measured values of the electrical A-f coefficient (κ_e). We observe strong scaling of this parameter, proportional to L^6. This

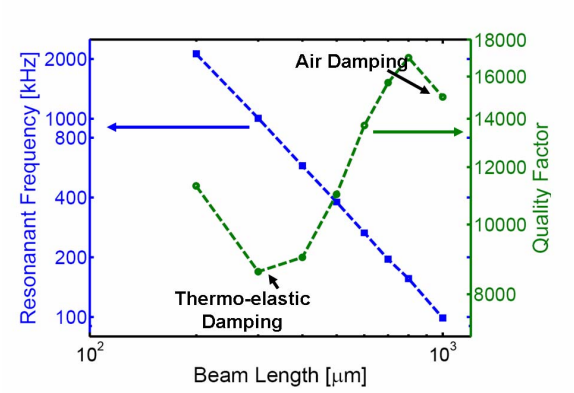

Fig. 2. Resonant frequency and quality factor measurements. $1/L^2$ scaling in the resonant frequency is evident.

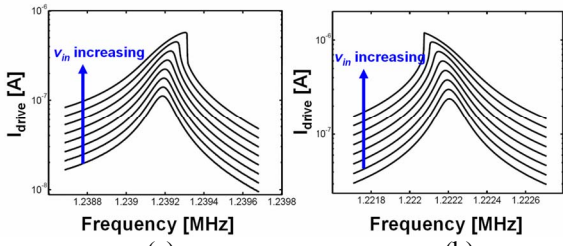

(a) (b)

Fig. 3. Measured frequency response distortion due to the A-f effect. a) Mechanical stiffening nonlinearities, at low V_{Bias} (13V) and b) Electrical softening at high V_{Bias} (60V).

TABLE 1. *Analytical models and scaling dependences on L for nonlinear and related properties in electrostatic MEMS resonators.*

Property	**Analytical Model**	***L*-dependence**
Resonant Frequency	$f_0 = \frac{\beta^2 w}{4\sqrt{3}\pi L^2}\sqrt{\frac{E}{\rho}}$	L^{-2}
3rd order beam Stiffness nonlinearity coefficient	$k_3 = 12.272\frac{Ehw}{L^3}$ (Ref. [7])	L^{-3}
Electrical A-f Coefficient	$\kappa_e = -\frac{3}{m\omega_0^4 \varepsilon A d}$	L^6
Optimal Bias Voltage	$V_{Bias,opt} \approx \sqrt{\frac{k_3 d^5}{4\varepsilon A}}$	L^{-2}
Bifurcation limited current handling	$I_{drive,opt} \geq \frac{2}{\sqrt{3\sqrt{3}\lvert\kappa_e\rvert Q}}$	L^{-3}

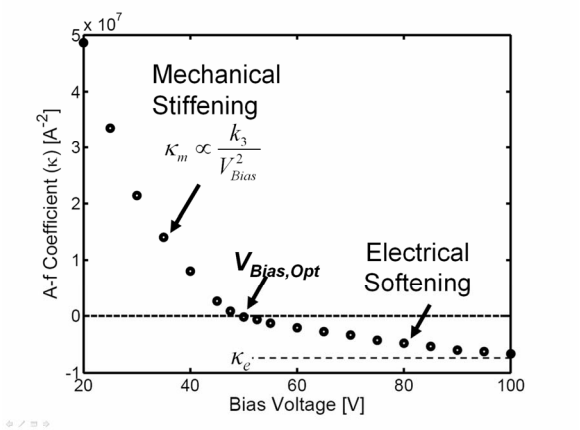

Fig. 4. Typical A-f coefficient dependence on V_{Bias}. Measurement shown here for an L = 200 μm DETF resonator.

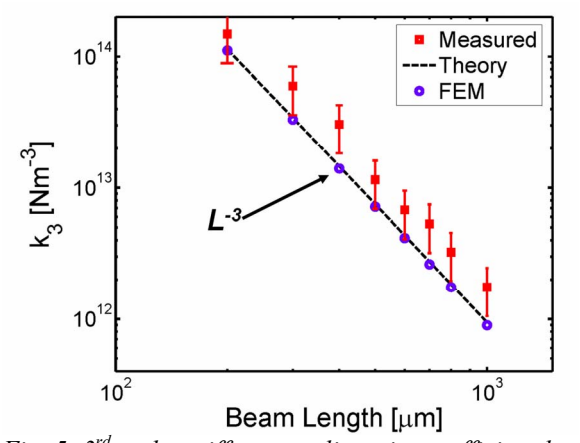

Fig. 5. 3rd order stiffness nonlinearity coefficient k_3 vs. beam length. The large error bars in the measured data are due to uncertainty in the gap size d (~0.1 μm).

dependence is due to the length dependence of resonant frequency (L^{-2}) and the ω_0^{-4} dependence of κ_e. It is important to note that compared to quartz (κ = 10^{-1} to 10^{-3} *Ampere*$^{-2}$), the presented MEMS resonators exhibit very high A-f dependence. However, unlike quartz they show very strong scaling of this parameter with resonant frequency. κ for quartz is essentially independent of frequency [2].

Fig. 7 shows the measured $V_{Bias,opt}$ for the resonators. By operating at $V_{Bias,opt}$, it is possible to balance the electrical and mechanical nonlinearities thereby increasing the current handling [6]. We see that this voltage scales according to the theoretically predicted L^{-2}. However, at small aspect ratios (shorter beam lengths) we begin to see some deviation from this behavior. This is most likely due to the departure from the long-slender beam or the perfectly clamped-clamped beam assumption made in the analytical models and FEM simulations.

Fig. 8 shows the measured maximum output

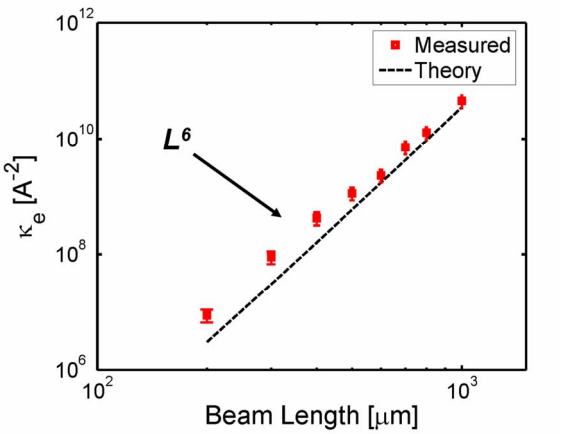

Fig. 6. Electrical A-f coefficient κ_e vs. beam length.

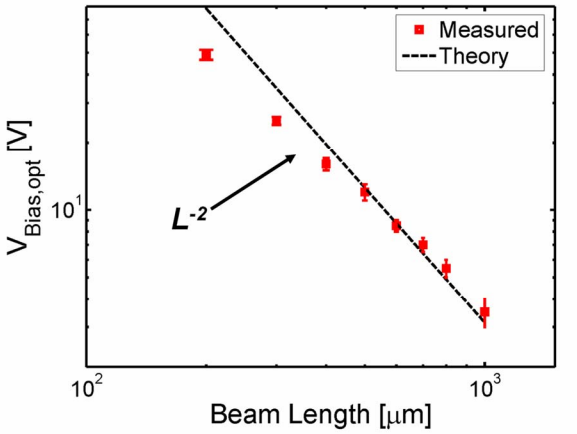

Fig. 7. Optimal bias voltage ($V_{Bias,opt}$)vs. beam length.

current at critical bifurcation [7, 8, 12] at $V_{Bias,opt}$. The predicted L^{-3} scaling is observed in this plot. Particularly, we find that the current obtained from the 1000 μm beam is about 100 times smaller than that of the 200 μm beam resonator.

4. DISCUSSION & CONCLUSIONS

It has previously been speculated that miniaturization in MEMS and NEMS resonators will lead to degradation in the phase noise performance, due to fundamental physical phenomena [13, 14]. Although these mechanisms will be relevant for very small resonators, the phase noise performance of practical realizations is typically limited by nonlinear effects and associated current handling bounds. Based on this work, we conjecture that proper scaling to smaller sizes can help improve current handling and hence phase noise performance.

The main findings of this paper, as they relate to device design and optimization are summarized as follows:

Optimization of Electrostatic Gap size (d) : Shorter

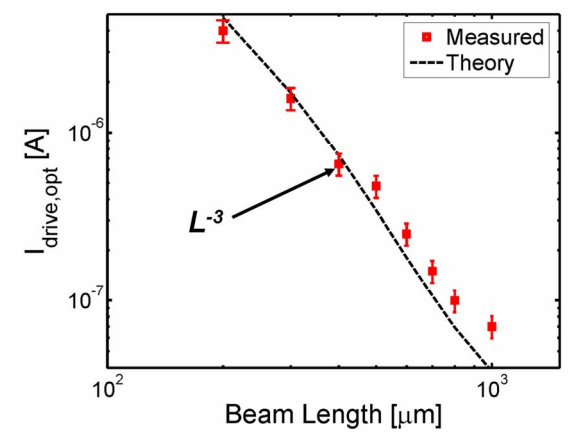

Fig. 8. Maximum output current $I_{drive,opt}$, or critical bifurcation current at V_{Bias} = $V_{Bias,opt}$ vs. beam length. The dashed line uses the expression for $I_{drive,opt}$ and κ_e given in Table 1 and experimentally measured values of Q. This represents the upper limit of available current ignoring nonlinearity reduction [6, 12].

beam lengths increase the available drive current but call for an undesired increase in $V_{Bias,opt}$. From the expressions presented in this paper, it follows that $I_{critical} \propto \sqrt{d}$ and $V_{Bias,opt} \propto \sqrt{d^5}$. Hence, by reducing *d,* it is possible to trade-off some of the signal current for a reduction in the required optimum bias voltage $V_{Bias,opt}$. Due to the increase in the nonlinearities of the electrical forces, very small gaps may lead to a situation where no optimum bias voltage is found.

Optimization of beam geometry: The observed scaling provides important design insight for dimensioning the beam resonators. To first order, the beams should be designed for the smallest possible aspect ratio (*L*/*w*). However very small *L*/*w* (approximately less than or equal to 10) may cause departure from the assumed resonant mode shape as the long-slender beam assumption breaks down.

Superior resonant structures: Compared to flexural beam type resonators (this work), bulk-acoustic-wave and similar resonators [7] can achieve higher frequency, higher effective mass and larger area of transduction simultaneously. Therefore, these structures have been shown to exhibit high current handling [7] (low κ_e, Table 1).

ACKNOWLEDGEMENTS

This work was supported by DARPA HERMIT (ONR N66001-03-1-8942), Robert Bosch Corp. (RTC) and the National Nanofabrication Users Network facilities funded by the National Science Foundation under award ECS-9731294, and The National Science Foundation Instrumentation for Materials Research Program (DMR 9504099).

The authors wish to thank Prof. David B. Leeson and Dr. John R. Vig for valuable discussions.

REFERENCES

[1] C. T.-C. Nguyen, "Vibrating RF MEMS technology: fuel for an integrated micromechanical circuit revolution?," presented at Solid-State Sensors, Actuators and Microsystems (Transducers'05), 2005.

[2] J. J. Gagnepain, "Nonlinear Properties of Quartz Crystal and Quartz Resonators: A Review," presented at IEEE Frequency Control Symposium, 1981.

[3] W. H. Horton, et al., "Dynamic measurement of amplitude-frequency effect of VHF resonators," *IEEE Transactions on Ultrasonics, Ferroelectrics and Frequency Control*, vol. 53, pp. 159-166, 2006.

[4] M. Agarwal, et al, "Nonlinear Characterization of Electrostatic MEMS Resonators," presented at IEEE Frequency Control Symposuim, Miami, FL, 2006.

[5] R. N. Candler, et al, "Long-Term and Accelerated Life Testing of a Novel Single-Wafer Vacuum Encapsulation of MEMS Resonators," *IEEE Journal of Microelectromechanical Systems*, 2006.

[6] M. Agarwal, et al, "Optimal drive condition for nonlinearity reduction in electrostatic microresonators," *Applied Physics Letters*, vol. 89, no. 21, 214105, 2006.

[7] V. Kaajakari, et al, "Nonlinear limits for single-crystal silicon microresonators," *Microelectromechanical Systems, Journal of*, vol. 13, pp. 715-724, 2004.

[8] L. D. Landau and E. M. Lifshitz, "Resonance in non-linear oscillations," in *Mechanics*, vol. 1, *Course of Theoretical Physics*, 3 ed. Reading, MA USA: Butterworth-Heinemann, 1982, pp. 87-92.

[9] B. Kim, et al, "Temperature dependance of quality factor in MEMS resonators," presented at MEMS'06, Istanbul, Turkey, 2006.

[10] R. N. Candler, et al, "Impact of Geometry on Thermoelastic Dissipation in Micromechanical Resonant Beams," *JMEMS*, 2006.

[11] URL: http://www.comsol.com/.

[12] M. Agarwal, et al, "Non-Linearity Cancellation in MEMS Resonators for Improved Power-Handling," presented at IEEE International Electron Devices Meeting, Washington D.C., USA, 2005.

[13] K. L. Ekinci, et al, "Ultimate limits to inertial mass sensing based upon nanoelectromechanical systems," *Journal of Applied Physics*, pp. 2682-2689, 2004.

[14] J. R. Vig, et al, "Noise in microelectromechanical system resonators," *IEEE Transactions on Ultrasonics, Ferroelectrics and Frequency Control,* vol. 46, pp. 1558-1565, 1999.